Available online at www.sciencedirect.com
ScienceDirect
Trans. Nonferrous Met. Soc. China 33(2023) 254−274
Transactions of Nonferrous Metals Society of China
www.tnmsc.cn

Influence of sensor array on MS/AE source location accuracy in rock mass

Lin-qi HUANG, Xin WU, Xi-bing LI, Shao-feng WANG

School of Resources and Safety Engineering, Central South University, Changsha 410083, China

Received 7 May 2022; accepted 21 October 2022

Abstract: As the mining depth increases, rock dynamic disasters become increasingly prominent. Microseismic monitoring has become an important technical means to monitor rock dynamic disasters, such as rockburst and roof collapse. The sensor array is the first step of signal acquisition and will seriously affect source location accuracy. The significant studies on error factors caused by sensor array arrangement to the location accuracy of microseismic (MS) and acoustic emission (AE) sources were discussed and summarized. The influences of the number of sensors, configuration of sensors and distance between sensors and source on MS/AE source location accuracy were analyzed. Subsequently, some principles of sensor arrays were given by combining with engineering practices and laboratory testing, and confirmed by a field application. In addition, the optimal arrangement scheme was discovered by considering the factors affecting the number, shape, and distance of sensors, which can greatly adjust the signal acquisition effect and improve the source location accuracy. Finally, some challenges and the corresponding coping strategies of sensor arrays were prospected to improve the MS/AE source location accuracy.
Key words: microseismic monitoring; acoustic emission; sensor array; source location accuracy

1 Introduction

The phenomenon where elastic strain energy is released when the material is fractured or deformed by external or internal forces is described as acoustic emission activity (acoustic emission, AE) [1−3]. However, in studies examining damage and failure of materials, such as coal and rock masses, rock fracture or crack propagation is described as microseismic activity (microseismic, MS) [4−6]. The AE and MS are fundamentally similar in terms of monitoring techniques and analytical theory [7]. The AE/MS signals generated during underground rock mass failures contain a significant amount of information about the fracture development and failures of surrounding rock, so the spatial structure and location of seismic sources can be determined [8−10]. The AE/MS source location refers to the use of sensor spatial coordinates, acoustic arrival times, acoustic propagation speeds, waveform pickup signals, and other parameters in the source location algorithm to get the structures and locations of rock fracture sources [11−18]. The AE/MS source location is an important task in the AE/MS monitoring technologies to predict and determine the rock fracture and failure in laboratory tests and on-site observations in underground mining, tunnelling and other rock excavations, which is significantly influenced by rock properties, geological conditions, and sensor parameters and layouts.

In recent years, many scholars have made efforts to further seismic source location. HUANG et al [19−21] proposed a method to calculate time differences based on cross wavelet transformation for positioning errors caused by inaccurate time difference pickups. By comparing the energy on the cross-wavelet spectrum and automatically selecting homologous signals, the accuracy for time difference pickups was effectively improved. However, this method did not consider the influence of seismic

Corresponding author: Shao-feng WANG, Tel: +86-18073369486, E-mail: sf.wang@csu.edu.cn
DOI: 10.1016/S1003-6326(22)66104-1

wave propagation time history. WU et al [22,23] proposed deconvolution migration by combining deconvolution interferometry with interferometric cross-correlation migration to improve the accuracy for locating microseismic events. SCHUSTER et al [24] used interferometric seismic imaging to image source locations or reflectivity distributions from passive seismic data where the source position or wavelet is unknown. XU et al [25] assumed that seismic waves propagated in straight lines and established a fast microsource location method based on the minimum travel surface method of seismic waves. For this method, the propagation path of seismic wave in three-dimensional space was transformed into a two-dimensional plane by rotating the coordinate system, and the layered characteristics of rock mass and the refraction of seismic waves in different media base planes were fully considered. The improved genetic algorithm was used to optimize the microsource stability in the three-layer horizontal model. But in practice, seismic wave propagation paths are not straight lines, meaning certain positioning errors will occur. LI et al [26] established a simplex microseismic source location method based on L1 norm statistics (minimum absolute value method) through the residual analysis of source location. This method took into account the errors inherent in input data, such as time and wave velocity, and ensured high stability and positioning accuracy. However, this method did not consider the effects of station layout on seismic location accuracy. Considering the influence from the combination of single-component sensors on source locations, DING et al [27] resolved the microseismic source location by using the inverse time-ray tracing method through the linear combination of two orthogonal single-component detectors, and this method was highly accurate and precise. In addition, noise exhibits a minor influence on the positioning results. However, the heterogeneity of geological strata will significantly interfere with the propagation of acoustic waves and thus affect the positioning results. ZHOU et al [28] proposed a method for acoustic emission source location considering the refractions of different media, and established the space−time relation equation between acoustic emission source points and measurement points. This algorithm only considered the refraction at the interface of two kinds of media. For more complex media, the applicability of the proposed method needs to be further verified. COLLINS et al [29] considered multiple geological units with complex shapes and simulated mining and geotechnical operations by adding multiple gaps, such as air, brine, or cement backfill, to analyze the impact of the rock mass velocity model on microseismic location accuracy. van DOKET et al [30] proposed anisotropic parameters to be captured in microseismic monitoring projects, which can and should be included in the final velocity model to obtain more accurate event locations. By exploring three-dimensional non-uniform structure sound source positioning, YIN et al [31] proposed triangular pyramidal sensor cluster for positional technology. The differences in signal times between different sensors are analyzed, and the refraction effect of acoustic waves in non-uniform medium was considered, which can achieve rapid and accurate sound source locating, but there are some geometric limitations in the actual sensor arrangement, which affect the source location precision.

From the above literatures, it can be seen that source location accuracy depends on many factors, such as an optimal layout for the spatial network of the microseismic network, anisotropic parameter and model of rock mass and velocity model of wave propagation, time pickup, and seismic wave location algorithm. According to the field measurement results, although the positioning accuracy of the existing acoustic emissions or microseismic monitoring system in the horizontal direction can be precise down to the meter, the positioning errors in the vertical direction are tens of meters, even hundreds of meters, which still falls below the needs of safe production in terms of overall positioning accuracy. The design of sensor array, its size, geometry, and quantity of the site layout range, significantly influences the accuracy of seismic source location. When planning and laying out arrays, the number of arrays and their arrangement in the monitoring area are crucial for the signal acquisition stage and the subsequent analysis of seismic source locations and mechanisms.

The research purposes for the sensor array in MS/AE are primarily to study the seismic activity and tectonic activity process within the region and to determine seismic source locations. However,

most of the current research is focused on improving the source location algorithm and intelligent signal recognition. There is lack of literature to summarize the studies on optimal sensor array arrangements and their influence on location accuracy. The rationality of sensor array placement greatly affects the validity of data acquisition and error accuracy in data processing, which is for studying rock fracture mechanisms and seismic source locations.

2 Accuracy analysis of array layout in MS/AE source location

The sensor array is composed of a certain number of sensors arranged in a certain network around the source. When acoustic emission or microseismic signals appear in the monitoring area, the sensors can pick up these signals and collect and measure signal timing information according to multi-sensor synchronization data. Then, combined with the coordinates of each sensor and the measured wave velocities in advance, the location algorithm is used to locate the source and determine its temporal and spatial parameters [32,33].

When locating the source, the rock mass is regarded as anisotropic body, and then the source location can be expressed by sensor coordinates, wave velocity, and initial arrival time, as shown in the following formula:

$$(x_i-x)^2+(y_i-y)^2+(z_i-z)^2=(t_i-t)^2v^2 \quad (1)$$

where (x_i, y_i, z_i) are the coordinates of the sensor, (x, y, z) are the coordinates of the source, v is the average speed of stress wave propagation, t is the time when the rock mass breaks, and t_i is the time when the sensor receives the stress wave. A common method to determine the source location is to apply least square fitting to the arrival time of the observed stress waves. By giving a set of arrival times and assuming the seismic wave propagation model, a position can be solved to minimize the error between the measured arrival time and the arrival time calculated using the assumed position. It can be expressed as

$$T_i=T_i(\boldsymbol{\theta},\boldsymbol{p})+t_0 \quad (2)$$

where $\boldsymbol{\theta}$ is the vector of unknown parameters (x, y, z, t), T_i is the propagation time from the source to sensor i, and t_0 is the origin time. The set of sensors is $\boldsymbol{p}$=[p_1, p_2, ⋯, p_N].

The common objective function for determining the source location is to calculate the sum of squares of the difference between the arrival time and observed arrival time,

$$\Theta=\sum_{i=1}^{N}r_i^2 \quad (3)$$

where r_i is the difference between the arrival time and observed arrival time.

The solution that minimizes the aforementioned equation is called the least square solution. Because the source position parameters are nonlinear functions, the optimization problem is nonlinear. Geiger is the most commonly used method for minimizing the objective function for seismic location, and it employs the iterative Gauss-Newton method [34]. The new source position parameter estimation is obtained by finding the adjustment function and adding it to the test position, thus reducing the objective function, which is calculated as follows:

$$\Theta(\boldsymbol{\theta}^*)=\boldsymbol{r}^{\mathrm{T}}\boldsymbol{r} \quad (4)$$

$$\boldsymbol{\delta}(\boldsymbol{\theta})=-(\boldsymbol{A}^{\mathrm{T}}\boldsymbol{A})^{-1}\boldsymbol{A}^{\mathrm{T}}\boldsymbol{r} \quad (5)$$

where $\boldsymbol{\theta}^*$ represents the parameter of the new source location, $\boldsymbol{\delta}(\boldsymbol{\theta})$ represents an adjustment vector, $\boldsymbol{r}$ is the column vector containing N residuals, and $\boldsymbol{A}$ is the partial derivative matrix of the travel time at the estimated source.

According to the hyperbolic governing equation of source location, the hyperbolic shape of the source location depends only on the product of the difference between wave velocity and arrival time. The influence from error accuracy caused by time and speed is shown in Fig. 1. As the source distance outside the sensor array is longer than the distance inside the sensor array, the arrival time error is amplified, and the source location error outside the array is amplified. At the same time, when there is an error in the wave velocity model adopted for positioning, the influence on the propagation path will be more distinct, which further aggravates the error influence caused by the long propagation distance [35−37].

Therefore, the station layout crucially influences the positioning effect, and the station layout is often adjusted and optimized according to the advantages and disadvantages of the positioning effect in actual positioning [38]. Usually, the plane focal position can be determined by the S wave, P

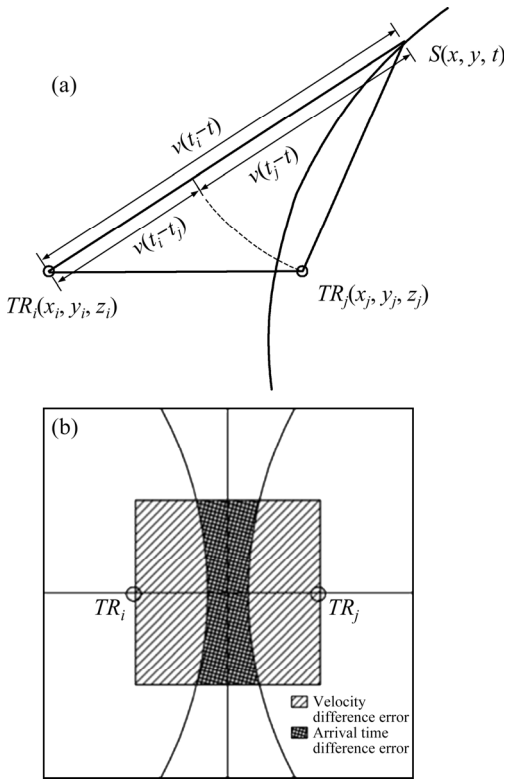

Fig. 1 Analysis of source location error: (a) Sensor positioning principle; (b) Enlarged view of positioning error

wave, and velocity collected by the three stations. However, if the three stations are distributed in a straight line, one epicenter locus line can be determined for every two stations as a group. Because the stations are distributed in a straight line and parallel to each other, the epicenter location cannot be determined. This kind of array layout is a typical "three-line" problem. Similarly, if there are four stations, it is generally able to determine the source location. But if the four stations are distributed on the circumference of a circle, every three stations can determine an epicenter trajectory line through the outer center of the three stations. Since the tables are distributed on a circle, the outer center of each group is the center of the circle. These epicenter tracks are a set of radiating lines passing through the center of the circle, and the location of the epicenter cannot be determined. Therefore, the spatial distribution and configuration of sensors will affect the positioning accuracy of microseismic events, and the quality of the sensor layout depends on the positioning error of their configuration. Considering the influence of sensor array flatness, LEANIAK et al [39,40] proposed the source location and location error evaluation method. The seismic source location accuracy of different sensor arrays was calculated by computer simulation and tested on the multi-layer rock mass model of the Lubin Copper Mine. Two different sensor arrays were installed. The first with uniaxial sensors spaced throughout the mine area, and the second with triaxial sensors mounted on the coal pan. The average error for the three-axis sensor positioning is at a minimum by employing the propagation time and direction of the seismic wave. Therefore, positioning errors can be used to measure the advantages and disadvantages of sensor arrangement. The previous studies showed that the absolute value method and least square method are commonly used in MS/AE positioning error calculation, and their calculation expressions are as follows:

$$\mathrm{Res}=\frac{\sum_{i=1}^{N}|r_i|}{n-m} \tag{6}$$

$$\mathrm{Res}=\left[\sum_{i=1}^{N}|r_i|^2\Big/n-m\right]^{1/2} \tag{7}$$

where Res represents the event residual, r_i is the residual associated with the ith station, N and n are the number of stations, and m is the degree of freedom. GE et al [36,41] analyzed and demonstrated the calculation accuracy for the absolute value method and least square method for station source locations. For the stations with major errors, the absolute value method has a superior residual retention ability, while the least square method tends to smooth out the residual errors from other stations, and positioning accuracy sensitivity decreases. In MS/AE source localization, the number of stations is usually quite small. The main error in source location is usually related to a few stations with errors originating from reading time and station coordinates. If the error is uncorrelated and random, the least square method is suitable; otherwise, the least square method will give improper weight to the data with large errors, which will distort the solution, and the error spreads to all stations. The location accuracy of the seismic source depends on the quality of input data, and the time correction value of relevant stations should be included in the additional parameters.

Currently, the D value theory and C value theory are widely accepted in network evaluation

methods to optimize the layout of the microseismic monitoring system. Both methods can evaluate the advantages and disadvantages of the network. According to the statistical theory of optimal experiment, KIJKO [42,43] first proposed a method to maximize the D-criterion for optimal sensor placement, namely the determinant of $\boldsymbol{A}^{\mathrm{T}}\boldsymbol{A}$, which can be defined as the objective function of maximization. For the seismicity area that needs to be monitored, it is divided into discrete areas first, and each area is assigned a weight. The weights assigned to a given zone are related to the probability of microseismic events. The locations of each partition, which are usually near the center, can be used to evaluate $\det|\boldsymbol{A}^{\mathrm{T}}\boldsymbol{A}|$. This value is then multiplied by the weight assigned to the partition, and the weighted sum is made so that the weighted and maximum configuration is the optimal placement method for the sensor. On this basis, GONG et al [44,45] applied and extended the theory of microseismic location and D value optimization design. Combined with the actual conditions of the coal mine, the main factors and unfavorable conditions affecting the location accuracy of mine earthquakes were studied. The general principle for determining the probability of occurrence of high microseismic activity areas and mine earthquake in coal mines by using comprehensive index method is posited. Through theoretical analysis into the weakness of the network location reflected by epicenter and source standard deviation, the expected value model of epicenter and source error based on the numerical simulation experiment method was established, and finally the network layout optimization and evaluation system were formed. MENDECKI [46] proposed the C-value theory to analyze the relationship between the network layout and the condition number of formed equations from the perspective of affecting the robustness of a nonlinear system, and evaluated the advantages and disadvantages of the network.

3 Influencing factor of array configuration on seismic location accuracy

3.1 Influence of sensor array scale

In practical applications, the array size of microseismic sensors deployed varies according to the nature of the project and scope of operation. The sensor array size depends on the scope of the monitoring area according to the development in existing microseismic monitoring technology [47]. This section discusses the engineering applications of microseismic technology in mining, oil and gas exploitation and seismic monitoring. For different scale engineering activities, the requirements for positioning accuracy are different [48−50]. In the field of mining, it primarily focuses on rock burst disasters in mines. The monitoring scope is at a certain mining stage. Due to economic or geological limitations, the number of sensors is few, which allows for small-scale microseismic monitoring and investigates small-scale rock fractures. For the microseismic events in the hydraulic fracturing process of oil and gas production, the ground surface or underground seismic array is used to monitor and determine the fracture trends and morphology of underground structures or fractured wells at different depths. The sensor array scale is larger than that in mining, and the scale of rock fracture is larger, which belongs to mesoscale microseismic monitoring [51]. In the field of seismic monitoring, the research primarily focuses on seismic disaster, geophysical exploration, and seismic wave attenuation law in rock strata, which is considered large-scale monitoring [52−53]. For different engineering projects, the sensor array size varies according to the monitoring scale, as shown in Fig. 2. For the same engineering project, the influences of different sensor array scales on the positioning accuracy are disparate. To meet the positioning accuracy requirements of the engineering, the optimized designs of sensor array scales can greatly save the cost. Thus, this paper analyzed typical engineering projects corresponding to the three scales, and compared the influences of the sensor array scales on positioning accuracy from the horizontal and vertical perspectives, as shown in Table 1.

The microseismic monitoring system was developed based on the seismograph network and seismograph array, which is used to study rock mass fracture deformations and stability. Among them, the MMS monitoring systems developed by ESG in Canada, ISS microseismic monitoring system in South Africa, SAK/SYLOK/SOS micro-seismic monitoring system in Poland, and CSIRO microseismic monitoring system of the Exploration

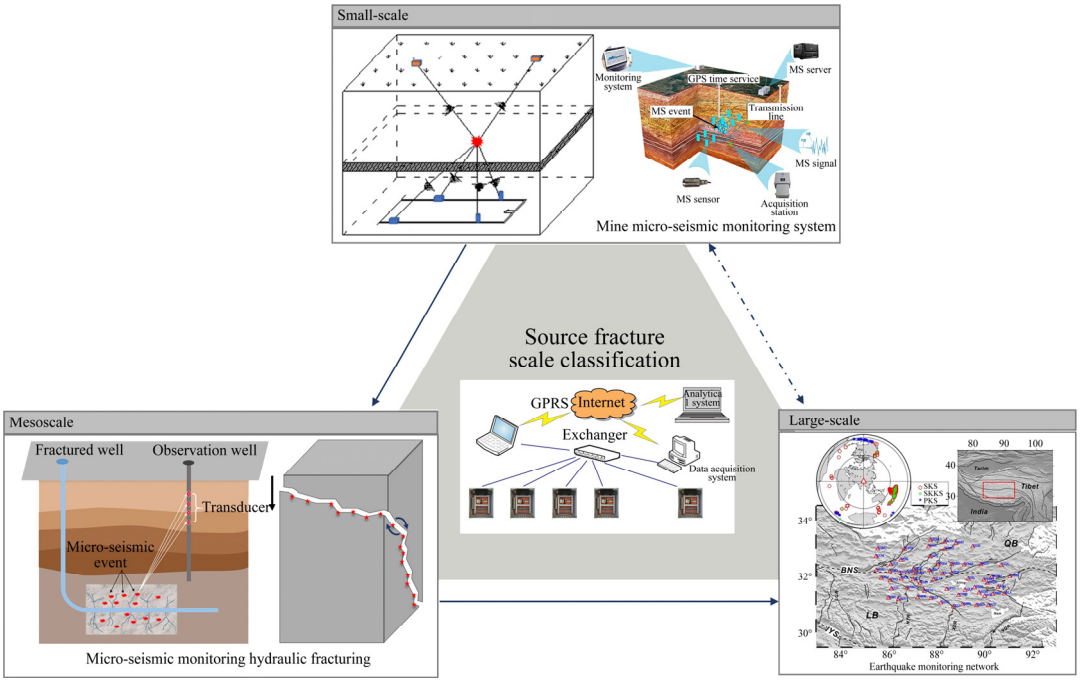

Fig. 2 Source fracture scale classification

and Mining Bureau of Commonwealth Scientific and Industrial Research Organisation (CSIRO) in Australia are more well-known. The monitoring system is widely used in rock burst monitoring in hard rock mines and coal mines. In the micro-seismic monitoring system, the sensor array scale varies depending on the engineering projects, and the positioning accuracy is also obviously different. The Beijing Mentougou Coal Mine introduced Polish SYLOK system in 1984. The monitoring area is roughly a narrow strip 6 km long and 3 km wide. The system has 8 stations, with a single station covering an area of 0.46 km^2, offering high station density and good positioning effect. In 1990, the Xinglongzhuang Coal Mine introduced a microseismic monitoring system from Australia and conducted experiments and research on microseismic monitoring to monitor and analyze the differences in underground stress field under different mining design conditions. Thus, the influence from sensor array scale layouts on monitoring and positioning results under different coal seam depths and mining designs was further explored. The early microseismic monitoring system was also called a geo-sound monitoring system. The information collected primarily includes the number of rock mass energy rates and events, but the positioning accuracy has not been studied further. Rock burst disasters in deep hard rock mine have unique microseismic activity. The rupture size (focal radius) is much smaller than a natural earthquake, the rupture time is short, the vibration frequency is high, and the source location accuracy is required to be high, so the positioning accuracy of early microseismic monitoring is nowhere near meeting the needs for detecting rockburst disasters. Dongguashan Copper Mine introduced the ISS microseismic monitoring system from the ISSI Company in South Africa in 2005. Considering the underground engineering conditions of the mine, TANG et al [56] adopted two hardware configuration schemes of 16 seismic sensors and 20 seismic sensors, and the results indicated that both schemes met the requirements for microseismic monitoring of the mine. However, compared with the former, the accuracy and system sensitivity of the latter showed no significant improvements. When considering the cost, it was more reasonable to adopt the hardware configuration scheme with 16 sensors, and the positioning error would be less than 5 m. Similarly, The Canadian ESG microseismic monitoring system MMS was introduced to the Fankou Lead−Zinc Mine in 2004. The arrangement scheme of 16 sensors was adopted, and the positioning error was within 5 m, so the monitoring effect was satisfactory. In 2019, the Tonglushan Copper Mine adopted the SSS microseismic monitoring system

Table 1 Summary of sensor array scale

Micro-seismic scale	Example projects	Monitoring scope	Microseismic monitoring system	Sensor array scale	Location error
Small-scale	Mentougou Coal Mine [54]	Mentougou Mine is 6 km long, 3 km wide, and 8 km deep	Poland SYLOK microseismic monitoring system	8 stations are arranged, wired transmission is employed, and maximum transmission distance is 10 km	Range of positioning error is large, ranging from 10 to 200 m
	Xinglongzhuang Coal Mine	Thickness of quaternary strata in microseismic monitoring area of mine is about 210 m; Coal seam being mined on working face is 3 layers of coal, elevation of coal seam ranges from −300 to −400 m, and thickness of coal seam ranges from 8 to 10 m	Australian earthquake monitoring system	According to depth position, 3 boreholes and 4 shallow holes were specially constructed, a total of 12 three-component geophones were installed, and 9 single-component geophones were arranged on ground	Determine fault zone and caving zone in coal mine production
	Fankou Lead−Zinc Mine [55]	For ore-bodies below 500 m and above −650 m, shilling north of main mining stope	Canadian ESG microseismic monitoring system−MMS	Full font 64-channel microseismic monitoring system (currently 16 channels open) has opened 16 channels, carrying 16 uniaxial sensors	<5 m
	Dongguashan Copper Mine [56]	First mining area and mining influence area; first mining area is located in 52−58 exploration lines, ore section above −850 m elevation	ISS microseismic monitoring system, ISSI South Africa	Sixteen seismic sensors were used, including four three-way sensors and 12 unidirectional sensors	<10 m
	Tonglushan Mine [57]	In middle section of −785 m and −845 m, actual monitoring depth can reach from −725 to −1120 m	Chinese Academy of Sciences SSS microseismic monitoring system	16-channel deep low-pressure microseismic monitoring system has 10 unidirectional sensors and 2 tridirectional sensors	<20 m
Meso-scale	Horizontal wells in Daqing SZ exploration area [58]	Fracturing depth in horizontal section of well ranges from 2025 to 2895 m, and vertical depth ranges from 1789.7 to 1794.2 m, with 23 perforating points in 11 stages	–	Ground monitoring has adopted six-arm star array with 66 receivers; 106-star observation systems are used for fracture imaging monitoring	25 m
	Biyang depression BYHF1 shale horizontal well segmentation [59]	AS1 Well has section of 2128−2458 m in 340 m east side	–	12-stage three-component geophone was placed in 340 m section of AS1 Well for microseismic monitoring with interval of 30 m	<10 m
	Charlson oil field in Mackenzie County, North Dakota	Two vertical wells and two horizontal wells	–	Vertical array of 40 detectors is deployed in well, spaced 15 m apart	Depth and position are optimized
Large-scale	Inner Mongolia seismograph network [60]	Inner Mongolia	–	97 seismic stations (48 in district and 49 in neighboring provinces)	4.16 km
	Norwegian seismic array [61]	Hedmark, Tromos, and Finnmark	–	PS27 station near Hamar in south (NOA) and PS28 station in Karasjok in north (ARCES) are both in series of stations, including 42 and 25 sub-stations, respectively	–

developed by China, with a positioning error within 20 m, which met the mine prediction needs. As equipment, instruments, and information technology have continued to develop, downhole rockburst and other disasters have developed from uncontrollable to controllable and predictable, effectively ensuring safe and efficient mining.

The microseismic activity generated by oil and

gas exploitation primarily occurs in the fracturing process of horizontal wells. Based on the principle of microseismic positioning, sensors are arranged in the space near the monitoring area to collect the microseismic information generated by rock fractures, and then the data are processed and used to source locations to locate rock fractures to study the geometry and extension direction of fractures after hydraulic fracturing. For low permeability oil and gas fields, hydraulic fracturing is a widely used measure for exploitation. The quality of fracturing and fracture development degrees are important for oil and gas development projects [62,63]. Since the beginning of the 21st Century, microseismic has received extensive attention in dynamic research of oil field production, and many domestic oil fields began to introduce hydraulic fracturing micro-seismic monitoring technology. Considering the development of low permeability reservoirs, the micro-seismic monitoring method has been used to monitor and evaluate the construction effect of water injection fracturing in the Changqing Oilfield and Jilin Oilfield, and considerable effects have been achieved [64−66]. Because of the shale deposit in the Biyang depression fracturing, ZHANG et al [67] deployed the horizontal well BYHF1 with the shale as the target layer, and used microseismic monitoring technology to conduct on-site real-time monitoring of the fracturing. In the 340 m section of the eastern part of the well, a 12-stage three-component geophone was placed for microseismic monitoring with an interval of 30 m. The strike, width, and height of the fracture network were studied. The results showed that the total effective fracturing volume was 3883×104 m^3, and the total fracture orientation was 34° north by east, which has achieved satisfactory microseismic monitoring. LIU et al [68] monitored the fracturing process of a shale gas reservoir in southwestern China by using relatively dense ground seismic stations, which can reliably determine the high-resolution, three-dimensional shear velocity results of the surface, thus improving the accuracy of positioning results.

Seismograph networks have been built in many places in China for areas that experience a high frequency of earthquakes. Inner Mongolia seismograph network can receive waveform data from 97 stations. The Inner Mongolia seismic network currently judges the accuracy of seismic location by fitting residuals. Based on this, ZHAO et al [60] selected 55 earthquakes with magnitudes greater than three in central and western Inner Mongolia and adjacent areas. By adjusting the station configuration, two station distribution modes of 7−14 stations and 4−9 stations were used to analyze the locations of the central and western regions. Among them, the results of 7−14 stations participating in seismic locations were relatively stable, and did not negatively affect the timeliness requirements for earthquake rapid reports. The monitoring effects of seismic networks are greatly affected by the location accuracy of seismic sources, and practical network layouts can improve location accuracy. KRAFT et al [69] proposed a network optimization method for regional scale micro-seismic monitoring based on existing seismic stations in northeastern Switzerland. The simulated annealing algorithm was used to optimize the geometric configuration of 10−35 stations, and the stability of the optimization results was satisfactory.

ZHAO [70] verified the influence of station density on microseismic positioning accuracy, and selected different sensor amounts for unknown wave velocity positioning. The positioning errors obtained are shown in Table 2. Theoretically, the more the stations are involved in positioning, the more in-depth the information is provided, and the higher the positioning accuracy is. Moreover, when more stations are involved in locating, the seismic

Table 2 Variations in positioning accuracy with number of stations

Number of stations	Error	Number of stations	Error
4	47.049	17	3.921
5	36.878	18	3.765
6	22.840	19	3.594
7	14.463	20	3.411
8	9.455	21	3.294
9	7.994	22	3.164
10	6.341	23	3.101
11	5.388	24	2.953
12	4.969	25	2.922
13	4.626	26	2.828
14	4.459	27	2.763
15	4.313	28	2.659
16	4.117	29	2.596

source envelope of the pickup is much improved, which offsets part of the error caused by the randomness of manual first arrival pickup and the inaccurate velocity model. However, the increase in the number of stations will inevitably lead to an increase in the number of problem channels. Therefore, appropriately increasing the number of location stations can improve location accuracy and ensure the stability of location results to a certain extent.

3.2 Influence of geometric layout of sensor array

The geometry of sensor arrays will affect the differences in the signal bunching ability. To achieve more accurate detection and recording of weak microseismic signals with strong background noise, the high sensitivity instruments are needed, and the densely distributed sensor arrays with specific geometric shapes are needed to enhance the signal clustering ability and achieve the waveform stacking effect [71]. The detailed features of the seismic source at the sensor array location can be extracted by frequency−wave number (F−K) analysis to extract the azimuth and phase velocity of seismic coherent wave trains as a function of frequency. The result showed that this processing method can improve event location accuracy [72,73]. Assuming that the array is in XOY plane, Fourier transformation can be used to decompose the given wavelength into plane waves

$$f(x,y,z)=\frac{1}{8\pi^3}\iiint f(k_x,k_y,\omega)\exp(ik_x x+ik_y y-i\omega t)\mathrm{d}k_x\mathrm{d}k_y\mathrm{d}\omega \tag{8}$$

where $f(k_x, k_y, \omega)$ is the frequency−wave number spectrum; $k_x=(\omega\cos\alpha)/V_a$, and $k_y=(\omega\sin\alpha)/V_a$, which represents the amplitude and phase of a plane wave propagating in the x−y plane with the apparent velocity value V_a and in the direction of azimuth angle α, and ω is the angular frequency. MO et al [74] proposed a frequency−wave-number based on the F−K energy bunching algorithm to pick up vibration signals in far fields of shallow underground sources. By establishing the evaluation index of the energy bunching effect, the bunching effects of different array geometry layouts are compared and analyzed. The results show that while picking up remote vibration signals, the alignment of regular hexagon array is the best. ROSACINTAS et al [75] analyzed the reliable dispersion curves provided by the minimum number of triangle stations, circle stations with center stations and polygon stations by combining F−K method. Polygon layouts do not have obvious center symmetry, while circular layouts or triangular geometric center symmetric theoretical arrays have satisfactory or acceptable dispersion curves, in which triangular arrays provide better results. Therefore, when the number of available stations is reduced, the geometric center symmetry of the response from the theoretical array should be maintained as much as possible, and the spatial continuity between the sensors should be maintained to obtain a better acceptable dispersion curve. OKADA [76] referenced the space autocorrelation (SPAC) method to derive the SPAC coefficient equation applicable to the data obtained from a circular array composed of a finite number of stations under the wave-direction constraints by using underground structure information. The SPAC coefficients for four different arrays were calculated according to these error terms, and the results showed that the three-station circular array was the best combination for effective microseismic observation using the SPAC method. For triangular or hexagonal arrays, which can generate independent SPAC coefficients in radial distances, ASTEN [77,78] discovered that the SPAC method can also provide sufficient azimuth coherence, which is conducive to the design of effective circular arrays.

Usually, the same number of different sensor arrays will achieve different results. For a two-dimensional plane, GE [35] enumerated three typical four-sensor arrays, as shown in Fig. 3. Through analysis and demonstration, the second type of sensor with a center station has better positioning accuracy. For a small-scale monitor network for regional seismic exploration, ARORA et al [79] used four (minimum) sensors in different triangular station arrays. It was shown that the equivalent length of a right triangle (three measuring points at the vertex and one near the center of mass) was the best source arrangement around the location network, which was equivalent to the radial distance to the epicenter. DENG [80] conducted regular triangle and square layouts, and the results showed that both met the minimum number of sensor records, but the square layout method used about 50% more stations than the

triangle layout method. For acoustic emission source locations of large plate structures, ALJETS et al [81] used three sensors to form a triangular sensor array. This configuration achieved the positioning accuracy and reduced the number of sensors needed for large structure monitoring. KIJKO and SCIOCATTI [82] analyzed the accuracies of seven different optimal seismic networks, which consisted of 4−10 stations. The greatest improvement in accuracy was achieved when a four-station network was replaced by one with five or six stations. Aiming at the scale and size of the sensor array in the microseismic system of the engineering project, CHEN and HUANG [83] designed the number and arrangement of 7 groups of stations, which were 4, 5, 9, 16, 25, 36, and 49, respectively. In the case of a certain Gaussian error, as the number of seismic stations increased, the positioning results were improved to varying degrees. In the vertical direction, station distribution with observation stations in the center greatly improved the depth location accuracy of microseismic events.

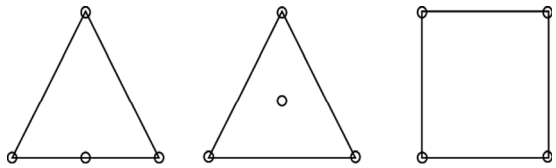

Fig. 3 Three typical sensor arrays: (a) Triangle with station at side center; (b) Triangle with center station; (c) Rectangle

For three-dimensional space, DONG et al [84−86] proposed a cube array arrangement of acoustic emission sensors to improve the accuracy of acoustic emission source location. PADOIS et al [87] proposed the optimal spherical microphone array geometry to improve noise impact. For source location, STEINBERG et al [88] designed networks of 6, 7, 8, 9, and 10 stations, and the optimal network was surrounding the potential source. This kind of network can reduce the statistical uncertainty and the random errors in arrival time, and can solve the multi-source location problem. According to the three-dimensional structure of the sensors installed on site, HUANG et al [19−21] proposed an intelligent algorithm for signal wave recognition, which showed that choosing mine positioning signals was closely related to sensor arrangements. ZHAO [70] compared the positioning effect of single plane and multi-plane monitoring, and found that the positioning effect of multi-plane monitoring was significantly better than that of single-plane monitoring. Thus, two sensor array schemes were designed to better explore the influence of sensor geometry layouts on seismic location accuracy. The improved Geiger algorithm was used to conduct acoustic emission source simulation experiments, and the results are shown in Figs. 4 and 5. Both schemes adopted three-dimensional space positioning, and the spatial geometries of the layouts were tetrahedron and triangular pyramid, and the undersides were triangle and square. The location results can be obtained by simulating acoustic emission sources from 6 aspects. The location accuracy of the tetrahedron with a quadrilateral base is higher than that of the triangular base, and the source envelope is better. Thus, choosing a reasonable sensor geometry layout scheme can improve source location accuracy.

3.3 Influence of distance between sensor and source

The propagation of vibration waves in rock mass will attenuate, so it is very important to study the optimal distances between sensor and source to determine positioning accuracy. The seismic waves collected from stations far away from the source travel a longer distance and pass through more geological discontinuities, and the attenuation and phase transformations of the waveform are more serious, leading to the possibility of waveform problems. This problem waveform will lead to inaccurate first-arrival pickup, which will affect the positioning accuracy. Therefore, the main factors affecting energy attenuation in seismic wave propagation are wave front diffusion and absorption diffusion [89,90]. In a uniform medium, the wave front of the point source is spherical. As the propagation distance increases, the spherical area also increases, but the total energy remains unchanged, so the energy per unit area of the diffusion surface decreases. The maximum amplitude of vibration is inversely proportional to the source distance, which can be expressed as

$$M = M_0/d \tag{9}$$

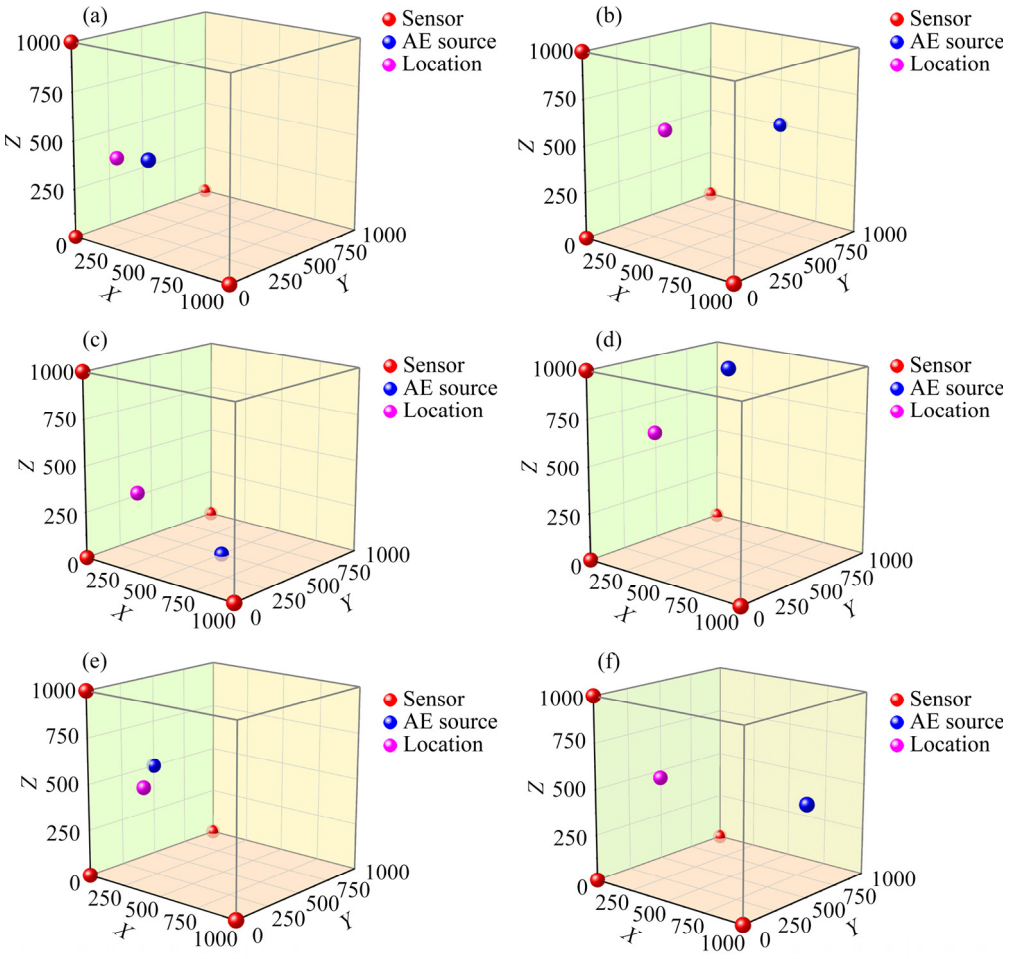

Fig. 4 Positioning results of three-dimensional space layouts of four sensors: (a) X–Z direction; (b) X'–Z' direction; (c) X–Y direction; (d) X'–Y' direction; (e) Y–Z direction; (f) Y'–Z' direction (X', Y' and Z' are the opposite directions of X, Y and Z, respectively)

where M is the maximum of the measured point, M_0 is the amplitude of the source, and d is the distance from the source.

Since the actual rock layer medium is not uniform, there are friction, liquid flow, viscosity tension, and so on in the propagation process, so the seismic wave produces attenuation, known as absorption attenuation. The attenuation rate of amplitude per unit distance can reflect the degree of absorption attenuation, which is expressed by absorption coefficient β. It is proven theoretically that the absorption coefficient is a function of frequency. For a certain rock medium, under the same amplitude, the higher the frequency is, the greater the absorption coefficients. Therefore, with the increase in seismic wave propagation distance, the high frequency part is quickly absorbed, and only the lower frequency component is retained, so the absorption coefficient is also a function of the source distance. The absorption attenuation of seismic waves is expressed as

$$M = M_0 \mathrm{e}^{-\beta(d)\cdot d} \tag{10}$$

The seismic wave is comprehensively influenced by wave front diffusion and absorption attenuation, and can be expressed as

$$M = \frac{M_0}{d} \mathrm{e}^{-\beta(d)\cdot d} \tag{11}$$

The β values are different at different source distances. The piecewise function is usually used to calculate the vibration attenuation law of natural earthquakes. In microseismic monitoring, the fixed β value is used in a certain range of source distance.

ZHAO [70] compared the mining blasting signal recorded by the instrument with the hammer

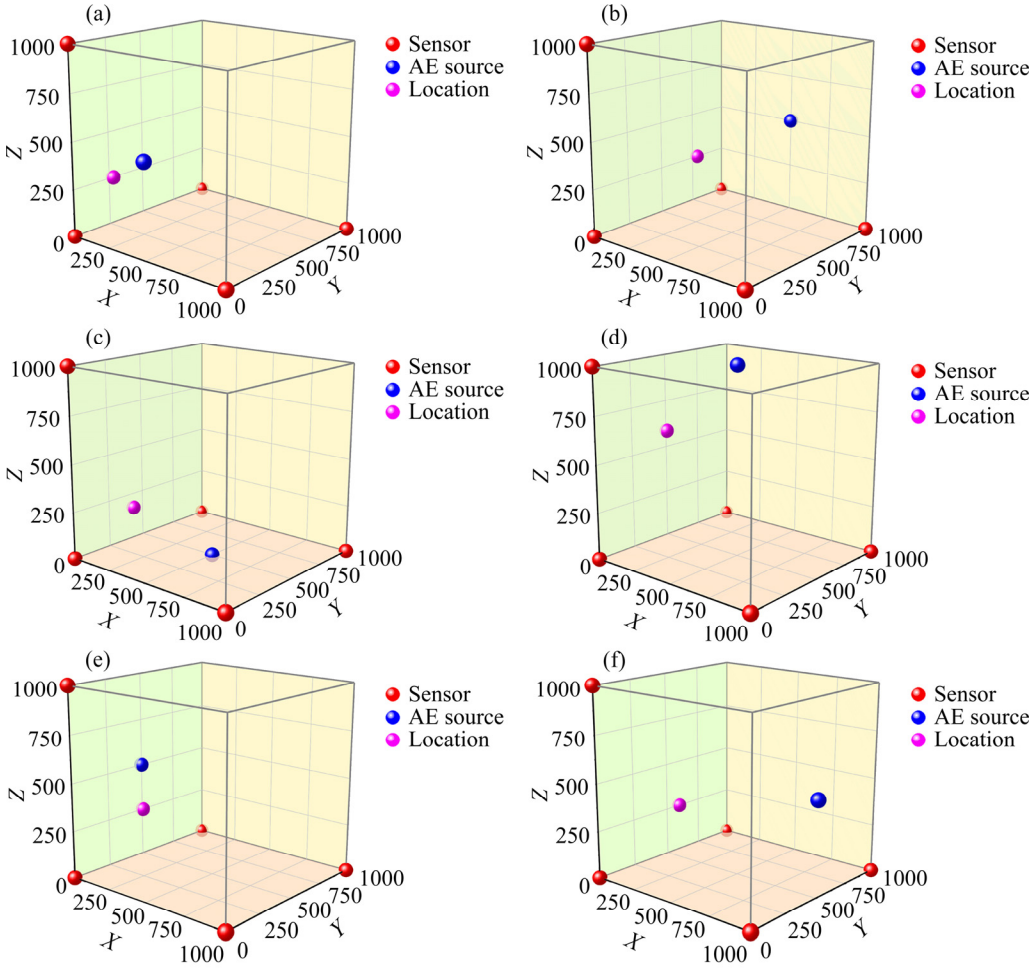

Fig. 5 Positioning results of three-dimensional space layouts of five sensors: (a) X−Z direction; (b) X'−Z' direction; (c) X−Y direction; (d) X'−Y' direction; (e) Y−Z direction; (f) Y'−Z' direction (X', Y' and Z' are the opposite directions of X, Y and Z, respectively)

test signal near a sensor. The results showed that the reception quality of the working face blasting signal received by the receiving sensor is better than the receiving effect of the micro-blasting signal within the sensor envelope, which indicates that the source distance has critical influence on the quality of the signal received by the sensor.

Through the acoustic emission simulation experiment of lead breaking, four sensor arrays at different distances were set on a rocky surface to locate the source. The positioning accuracies of the two methods with different distances were compared, as shown in Fig. 6. To explore the relationship between sensors and source distance, eight sensors were selected, and two sensor layout schemes were designed, including eight sensors with eight vertices and eight sensors evenly distributed on two planes, as shown in Figs. 7 and 8, respectively. In the two schemes, the positions of

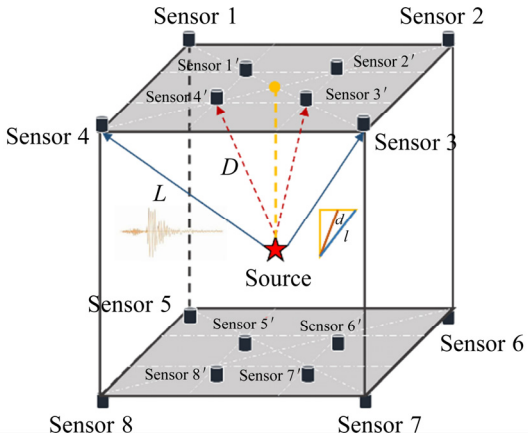

Fig. 6 Layout scheme of 8 sensors

acoustic emission source were unchanged, and the distance between source and sensor was different. The positioning errors obtained by using the Geiger method and Geiger-objective function method are given in Tables 3 and 4, respectively. Compared

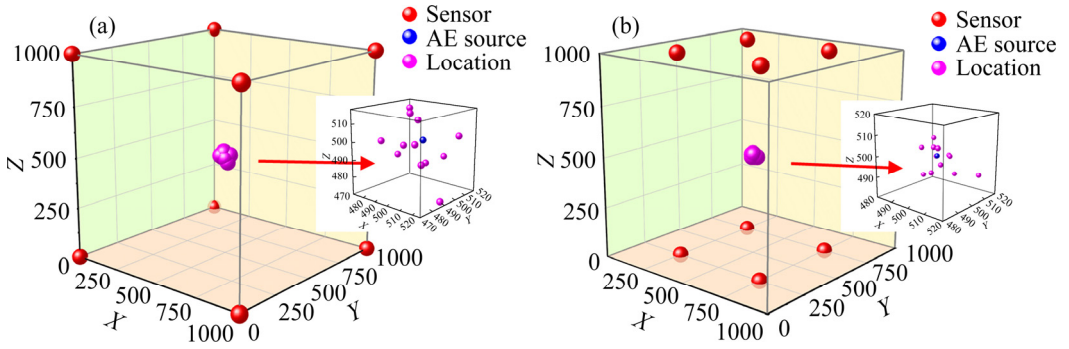

Fig. 7 Geiger location results from eight vertex sensors (a) and eight planar sensors (b)

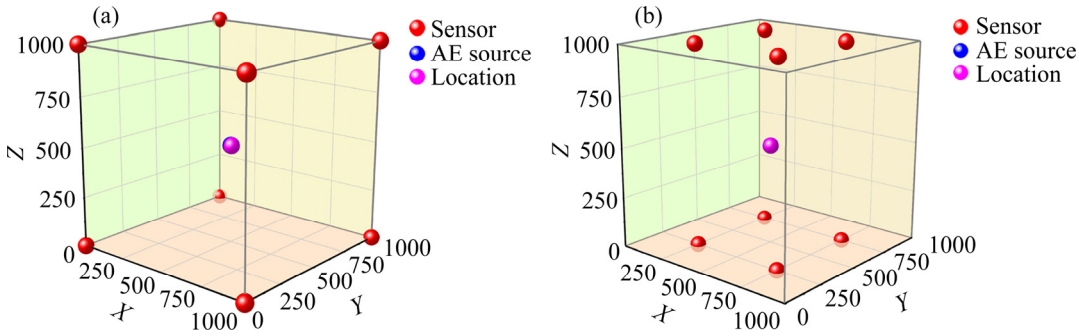

Fig. 8 Geiger-objective function location results from eight vertex sensors (a) and eight planar sensors (b)

Table 3 Location results of eight vertex sensors

Sensor location			Simulation of acoustic emission source location			Source location			Localization algorithm	Location error
X	*Y*	*Z*	*X*	*Y*	*Z*	*X*	*Y*	*Z*		
			500	500	500	496.2557	492.6423	515.7365		17.77053
			500	500	500	503.0593	489.3918	499.8823		11.04116
			500	500	500	518.9443	510.9099	502.9592		22.06062
0	0	1000	500	500	500	500.6789	501.8645	486.7316		13.41594
0	1000	1000	500	500	500	489.9943	498.9281	517.2643		19.98299
1000	0	1000	500	500	500	512.5025	484.5307	491.5067	Geiger method	21.62746
1000	1000	1000	500	500	500	520.5738	492.0819	470.6802		36.68278
0	0	0	500	500	500	481.1547	497.3068	489.6382		21.67403
0	1000	0	500	500	500	503.8154	515.7113	488.2087		20.01094
1000	0	0	500	500	500	498.01	497.6451	511.3779		11.78823
1000	1000	0	500	500	500	489.8935	493.57	496.8363		12.38931
			500	500	500	482.6634	481.9943	500.4164		24.99875
			500	500	500	507.5216	495.9189	500.6411	Geiger-objective method	8.58141

with the location results of the eight sensors at the vertex, the results indicated that the location accuracy of the eight sensors evenly distributed on the upper and lower surfaces is higher overall, indicating that the distance between sensors and source has a magnifying effect on the timing and velocity of source location error, thus affecting the location effect.

Table 4 Location results of eight planar sensors

Sensor location			Simulation of acoustic emission source location			Source location			Localization algorithm	Location error
X	*Y*	*Z*	*X*	*Y*	*Z*	*X*	*Y*	*Z*		
			500	500	500	503.72	498.0837	496.7888		5.274676
			500	500	500	501.9426	506.352	499.3518		6.674013
			500	500	500	502.5693	510.1015	489.0839		15.09311
250	250	1000	500	500	500	512.1033	486.0821	508.4074		20.27021
250	750	1000	500	500	500	506.0129	488.8743	495.5892		13.39367
750	250	1000	500	500	500	495.211	495.7927	490.7667	Geiger method	11.22009
750	750	1000	500	500	500	518.4263	507.3908	492.4486		21.24091
250	250	0	500	500	500	490.5153	508.7202	505.5005		14.00913
250	750	0	500	500	500	498.3927	501.2696	499.3172		2.159046
750	250	0	500	500	500	502.5053	494.5537	505.5491		8.168968
750	750	0	500	500	500	493.5592	496.4491	503.5922		8.185149
			500	500	500	504.3166	504.1029	499.6878		5.963604
			500	500	500	503.096	497.6284	501.0213	Geiger-objective method	4.031418

4 Influence mechanism of sensor array on seismic location accuracy

The sensor array has an important influence on the source location. For the monitoring area, the signal analysis collected by the sensor has different positioning accuracies for different source locations. The location error of the source inside the sensor array is much smaller than that of the source outside. When the source is far away from the center of the network, the positioning accuracy and stability tend to decrease. The decrease rate of location accuracy and stability increases sharply when the source reaches the outer region beyond the edge of the array.

There are three factors that affect the location accuracy of seismic sources, including the scale and geometry of the sensor array, and the distance between sensor and source. In terms of the sensor array scale, more sensors collect more in-depth information, and the corresponding positioning accuracy will be higher. But for practical engineering applications, the number of sensors is limited by the field. The number of stations on a single plane will not necessarily achieve effective source location, and the increase in the number of stations will inevitably increase the occurrence of the problem waveform and affect the accuracy of the source location. With the increase in the number of participating stations, the envelope effect of the key monitoring area is improved. Therefore, the positioning error can be reduced by increasing the number of stations appropriately to ensure the normal waveform of stations. For the location algorithm, increasing the number of stations involved in location will reduce the singularity of the source solution covariance matrix of nonlinear equations, and thus improve the convergence robustness of the iterative process of source solutions.

The geometry layout of the sensor array is expected to achieve the maximum and optimal monitoring range and accuracy with the minimum number of sensors. Different geometry layouts will change the stacking effect of the waveform by affecting the bunching ability of signals. Most studies observed that the triangle or hexagon array can provide sufficient azimuth coherence by analyzing and comparing the bunching effect of different array geometries. Meanwhile, the arrangement with the central station has a better bunching effect. Three-dimensional space sensor layout with a reasonable planning sensor layout can minimize the instrument and time errors. In addition, the three-dimensional layout can be

optimized to achieve the "envelope" effect of the source, which can greatly improve the source location accuracy.

The influence of the distance between sensor and source is reflected in the attenuation of source energy. Because rock mass failure is unknown and random, the signals collected from stations farther away from the source have a longer propagation distance. The signal waveform attenuation and phase transformation are serious, which influence the location accuracy of seismic sources significantly. According to the focal mechanism, some scholars have established the signal attenuation displacement equation to reveal the distance relationship between the focal signal and sensor to reasonably estimate the effective monitoring range and avoid the signal loss caused by energy attenuation in the wave propagation process as much as possible.

5 Field application

According to the actual requirement for ground pressure monitoring in the Linglong Gold Mine, the zone from −620 m level to −670 m within a 200 m-radius circular area was determined to be a main monitoring zone, and the monitoring sensor layout of S3, S4, S5, S8, S13, S17, S18, and S20 boreholes was selected to establish a microseismic monitoring network. The borehole parameters in the monitoring network are listed in Table 5. The installation process for putting sensors in borehole is shown in Fig. 9.

The location accuracy of the monitoring network was determined with the point-blasting test. The three blasting point positions were selected to make into seismic sources with deterministic time and location to measure location accuracy. The

Table 5 Borehole parameters in monitoring network

Level/m	No.	Horizontal coordinate/m		Azimuth/(°)	Dip/(°)	Depth/m	Diameter/mm
		X	*Y*				
−620	S3	46266.36	47601.46	178	45	3	60
−620	S4	46395.38	47539.82	10	45	3	60
−620	S5	46571.06	47623.01	270	45	10	60
−620	S8	46714.19	47554.48	184	45	10	60
−670	S13	46224.05	47572.77	99	5	10	60
−670	S17	46691.19	7619.83	135	5	3	60
−670	S18	46641.13	47529.85	24	5	10	60

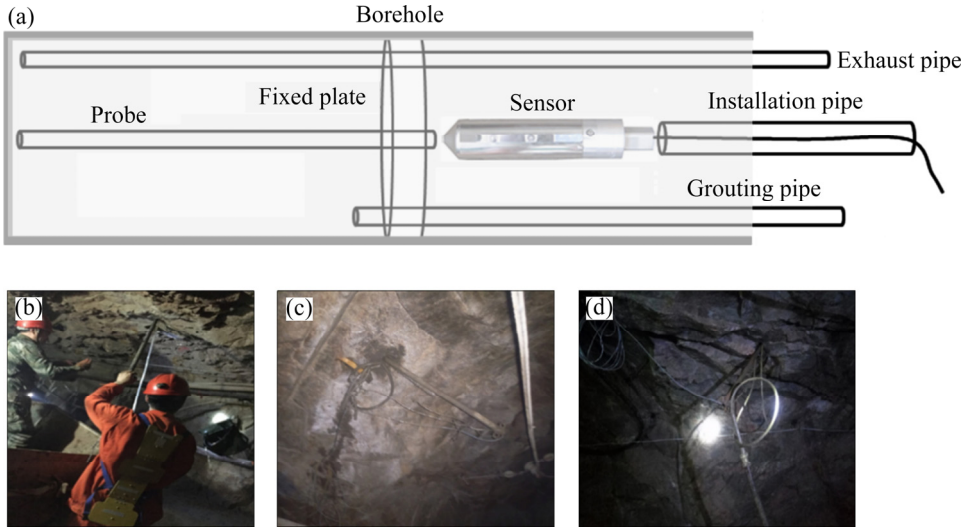

Fig. 9 Installation process of sensor in borehole: (a) Layout of sensor in borehole; (b) Importing; (c) Fixing and sealing; (d) Grouting

location results and the corresponding errors are listed in Table 6. The location errors of the selected monitoring network are 15−25 m.

The microseismic monitoring performance simulation analysis software, Ticker-3D, was used to analyze the location accuracy and sensitivity of the selected monitoring network. The cloud images of location accuracy and sensitivity are shown in Figs. 10 and 11, respectively. It can be seen that the location accuracy of the monitoring network in the

Table 6 Location accuracy in point-blasting test

No.	Blasting point coordinate/m			Location coordinate/m			*X*-direction error/m	*Y*-direction error/m	*Z*-direction error/m	Total error/m
	X	*Y*	*Z*	*X*	*Y*	*Z*				
1	46344.8	47651.3	−617.1	46362.6	47658.3	−610.5	17.8	7.1	6.5	20.2
2	46362.0	47610.9	−612.9	46348.4	47601.7	−610.0	13.5	9.1	2.9	16.6
3	46362.0	47620.9	−612.9	46347.5	47601.5	−610.3	14.4	19.3	2.6	24.3

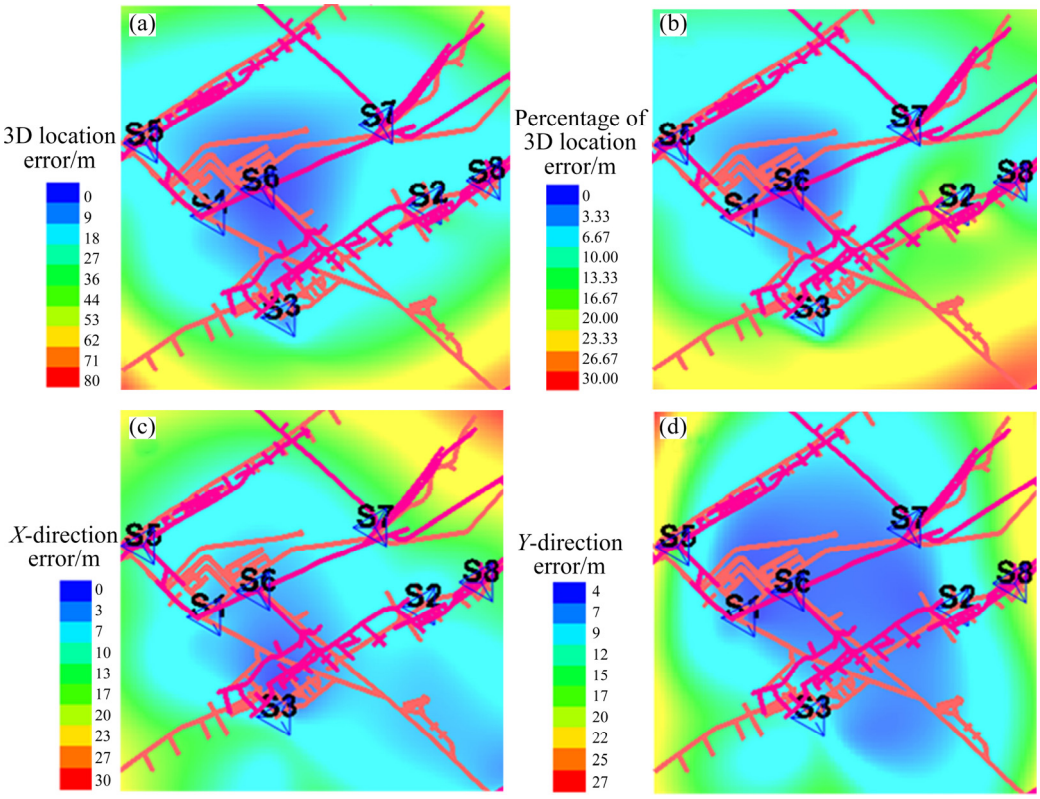

Fig. 10 Cloud images of location errors calculated from Table 6: (a) Three-dimensional location error; (b) Percentage of three-dimensional location errors; (c) *X*-direction location error; (d) *Y*-direction location error

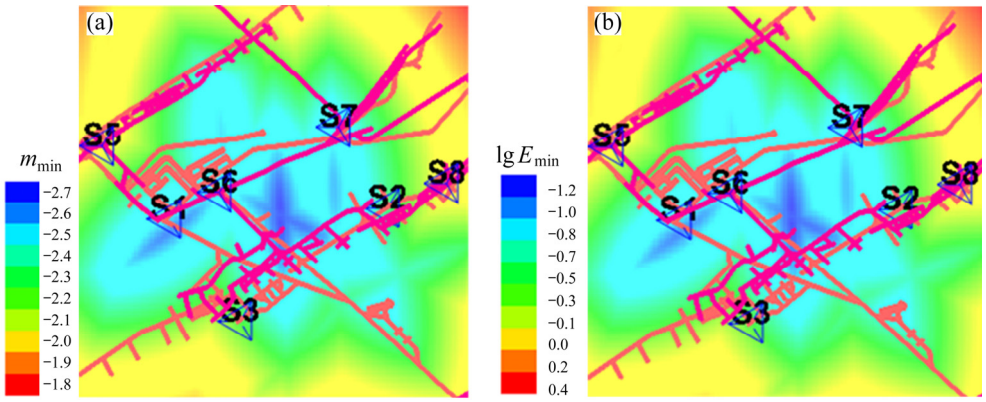

Fig. 11 Cloud images of sensitivities from Ticker-3D software: (a) Microseismic magnitude (m_{min}); (b) Microseismic energy (lgE_{min})

targeted zone is 9−27 m, and the sensitivities for monitoring microseismic magnitude and energy are from −2.6 to −2.1 and from −1.0 to 0.0, respectively. The results of the point-blasting test and simulation analysis are consistent. The layout of the monitoring network is reasonable, and its accuracy can meet the requirements for microseismic monitoring.

6 Prospects for sensor arrays

The reasonable arrangement of sensor array is an important guarantee for scientific design and adjustments of microseismic system construction. The location accuracy is significantly influenced by sensor array scale, sensor array geometry layout, and the distance between sensor and source. Based on the aforementioned analyses, the general principles for constructing sensor arrays are as follows: (1) The sensor array with more sensors presents a higher accuracy; (2) When selecting a small number of sensor layouts, the layout of the central station should be considered, which can greatly reduce the impact of sensor arrays and improve source location accuracy; (3) The sensor array should not be arranged on a single plane, and the sensors should not be arranged in a straight line or a shared circle, which easily causes positioning dead angles; (4) For engineering applications, the monitoring area should be surrounded as far as possible when selecting the monitoring range and arranging the measuring points before system installation, and the convenience of wiring and drilling should also be taken into account; (5) The size of the monitoring range should be commensurate with the number of selected sensors and the effective monitoring radius of each sensor to reduce the error impacts caused by distance attenuation.

Considering the particularity of source locations and the challenges facing sensor arrays, the current designs of sensor arrays for microseismic monitoring are primarily based on experience, or only considering simple factors, such as the number of stations and noise levels. With the gradual increase in major construction projects, the technical requirements for sensor array quantitative designs and signal acquisition optimization are increasing. This work summarizes the methods for sensor array optimization in the field of microseismic and acoustic emission from the perspective of positioning accuracy. The overall layout is shown in Fig. 12. Although it is preliminary, it can still provide some reference for promoting systematic layout optimization strategy. At present, most research on sensor arrays only focuses on the influence of sensor number and geometry. In future research, the sensor array should be reasonably optimized from the response parameters of the source, combined with the attenuation parameters of different strata. It can be expected to have a better signal acquisition effect and to achieve the maximum accuracy of the source location.

7 Conclusions

(1) The AE/MS signals contain significant information about the fracture and failure of rock mass in underground mining, tunnelling and other rock excavations. The AE/MS source location is an important task in the AE/MS monitoring

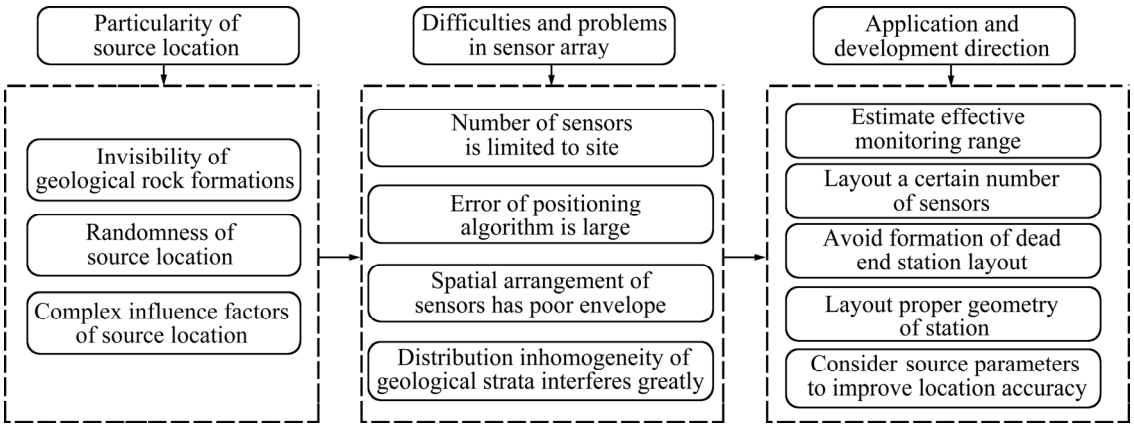

Fig. 12 Difficulties and prospects for sensor arrays

technologies to predict and determine the temporal and spatial characteristics of rock fracture and failure. Rock properties, geological conditions, and sensor parameters and layouts can significantly influence the location accuracy of AE/MS source. Specially, the sensor array is a key factor that can affect the source location accuracy and the subsequent source mechanism analysis.

(2) According the literature reviews, the influence factors of sensor array arrangement on the location accuracy of MS/AE sources were discussed and summarized, which referred to the sensor number, configuration of sensors and distance between sensors and source. In addition, the corresponding influence mechanism of sensor array on AE/MS location accuracy was analyzed and summarized to promote the understanding of the significance of sensor array.

(3) By combining example analyses and field observations, some principles and optimal arrangement scheme of sensor arrays were given to improve the location accuracy of AE/MS monitoring application. Finally, some challenges and the corresponding coping strategies of sensor arrays were prospected to address the particular problems.

Acknowledgments

The authors are grateful for the financial support from the National Natural Science Foundation of China (Nos. 51904335 and 52174098).

References

[1] LI Xi-bing. Rock Dynamic Fundamentals and applications [M]. Beijing: Science Press, 2014. (in Chinese)

[2] ZHANG Ru, AI Ting, GAO Ming-zhong, ZHANG Guo-qiang, ZHOU Cheng. Basic theory and experimental study of rock acoustic emission [M]. Chengdu: Sichuan University Press: 2017: 262. (in Chinese)

[3] LI Nan, WANG En-yuan, GE Mao-chen, LIU Jie. The fracture mechanism and acoustic emission analysis of hard roof: A physical modeling study [J]. Arabian Journal of Geosciences, 2015, 8(4): 1895−1902.

[4] LI Peng-xiang, FENG Xia-ting, FENG Guang-liang, XIAO Ya-xun, CHEN Bing-rui. Rockburst and microseismic characteristics around lithological interfaces under different excavation directions in deep tunnels [J]. Engineering Geology, 2019, 260: 105209.

[5] LI Yang, YANG Tian-hong, LIU Hong-lei, WANG Hong, HOU Xian-gang, ZHANG Peng-hai, WANG Pei-tao. Real-time microseismic monitoring and its characteristic analysis in working face with high-intensity mining [J]. Journal of Applied Geophysics, 2016, 132: 152−163.

[6] MA Tian-hui, TANG Chun-an, TANG Shi-bin, KUANG Liang, YU Qun, KONG De-qing, ZHU Xu. Rockburst mechanism and prediction based on microseismic monitoring [J]. International Journal of Rock Mechanics and Mining Sciences, 2018, 110: 177−188.

[7] WANG Hong-liang, GE Mao-chen. Acoustic emission/ microseismic source location analysis for a limestone mine exhibiting high horizontal stresses [J]. International Journal of Rock Mechanics and Mining Sciences, 2008, 45(5): 720−728.

[8] WANG Shao-feng, HUANG Lin-qi, LI Xi-bing. Analysis of rockburst triggered by hard rock fragmentation using a conical pick under high uniaxial stress [J]. Tunnelling and Underground Space Technology, 2020, 96: 103195.

[9] WENG Lei, HUANG Lin-qi, TAHERI Abbas, LI Xi-bing. Rockburst characteristics and numerical simulation based on a strain energy density index: A case study of a roadway in Linglong gold mine, China [J]. Tunnelling and Underground Space Technology, 2017, 69: 223−232.

[10] ZHAO Yong, YANG Tian-hong, ZHANG Peng-hai, ZHOU Jing-ren, YU Qing-lei, DENG Wen-xue. The analysis of rock damage process based on the microseismic monitoring and numerical simulations [J]. Tunnelling and Underground Space Technology, 2017, 69: 1−17.

[11] LI Yue. Study on seismic source information processing and inversion location method [D]. Xuzhou: China University of Mining and Technology, 2018. (in Chinese)

[12] LI Xiang, XU Nu-wen. Research developments and prospects on microseismic source location [J]. Progress in Geophysics, 2020, 35: 598−607. (in Chinese)

[13] DA Shu-jin, LI Xue-gui, DONG Hong-li, LI Han-yang. Summary of microseismic location methods [J]. Journal of Jilin University (Earth Science Edition), 2020, 50: 1228−1239. (in Chinese)

[14] TIAN Yue, CHEN Xiao-fei. Review of seismic location study [J]. Progress in Geophysics, 2002, 17: 147−155. (in Chinese)

[15] DONG Long-jun, ZOU Wei, SUN Dao-yuan, TONG Xiao-jie, LI Xi-bing, SHU Wei-wei. Some developments and new insights for microseismic/acoustic emission source localization [J]. Shock and Vibration, 2019, 2019: 9732606.

[16] JIANG Ruo-chen, DAI Feng, LIU Yi, LI Ang. A novel method for automatic identification of rock fracture signals in microseismic monitoring [J]. Measurement, 2021, 175: 109129.

[17] LI Yue, NI Zhuo, TIAN Ya-nan. Arrival-time picking method based on approximate negentropy for microseismic data [J]. Journal of Applied Geophysics, 2018, 152: 100−109.

[18] LIU Chao, LI Shu-gang, CHENG Cheng, CHENG Xiao-yu. Identification methods for anomalous stress region in coal roadways based on microseismic information and numerical simulation [J]. International Journal of Mining Science and Technology, 2017, 27: 525−530.

[19] HUANG Lin-qi, LI Jun, HAO Hong, LI Xi-bing. Micro-seismic event detection and location in underground mines by using convolutional neural networks (CNN) and deep

learning [J]. Tunnelling and Underground Space Technology, 2018, 81: 265−276.

[20] HUANG Lin-qi, LI Xi-bing, DONG Long-jun, ZHANG Chun-xuan, LIU Dong. Relocation method of microseismic source in deep mines [J]. Transactions of Nonferrous Metals Society of China, 2016, 26: 2988−2996.

[21] HUANG Lin-qi, HAO Hong, LI Xi-bing, LI Jun. Source identification of microseismic events in underground mines with interferometric imaging and cross wavelet transform [J]. Tunnelling and Underground Space Technology, 2018, 71: 318−328.

[22] WU Shun-chuan, WANG Yi-bo, ZHENG Yi-kang, CHANG Xu. Microseismic source locations with deconvolution migration [J]. Geophysical Journal International, 2018, 212: 2088−2115.

[23] WU Shao-jiang, WANG Yi-bo, XIE Fei, CHANG Xu. Crosscorrelation migration of microseismic source locations with hybrid imaging condition [J]. Geophysics, 2022, 87: KS17−KS31.

[24] SCHUSTER G T, YU J, SHENG J, RICKETT J. Interferometric/daylight seismic imaging [J]. Geophysical Journal International, 2004, 157: 838−852.

[25] XU Gang, XUE Chuan-rong, WANG Xin-ke, GAO De-jun. Microseismic Source location method considering refraction of seismic waves in layered media [J]. Chinese Journal of Rock Mechanics and Engineering, 2021, 40: 1654−1663. (in Chinese)

[26] LI Nan, WANG En-yuan, SUN Zhen-yu, LI Bao-lin. Simplex microseismic source location method based on L1 norm statistical standard [J]. Journal of China Coal Society, 2014, 39: 2431−2438. (in Chinese)

[27] DING Liang. LIU Qin-ya, GAO Er-gen, QIAN Wei, SUN Shou-cai. Locating microseismic sources based upon L-shaped single-component geophone array: A synthetic study [J]. Journal of Central South University, 2020, 27: 2711−2725.

[28] ZHOU Zi-long, ZHOU Jing, DONG Long-jun, CAI Xin, RUI Yi-chao, KE Chang-tao. Experimental study on the location of an acoustic emission source considering refraction in different media [J]. Scientific Reports, 2017, 7: 7472.

[29] COLLINS D S, TOYA Y, PINNOCK I, SHUMILA V, HOSSEINI Z. 3D velocity model with complex geology and voids for microseismic location and mechanism [C]// Proceedings of the Seventh International Conference on Deep and High Stress Mining. Australian Centre for Geomechanics, 2014: 681−688.

[30] van DOKET R, FULLER B, ENGELBRECHT L, STERLING M. Seismic anisotropy in microseismic event location analysis [J]. The Leading Edge, 2011, 30: 766−770.

[31] YIN Shen-xin, XIAO Hua-pan, CUI Zhi-wen, KUNDU T. Rapid localization of acoustic source using sensor clusters in 3D homogeneous and heterogeneous structures [J]. Structural Health Monitoring, 2021, 20: 1145−1155.

[32] LI Luo-lan, HE Chuan, TAN Yu-yang. Study of recording system and objective function for microseismic source location [J]. Acta Scientiarum Naturalium Universitatis Pekinensis, 2017, 53: 329−343. (in Chinese)

[33] LEE W H K, STEWARTS W. Principles and applications of microearthquake networks [M]. New York: Academic Press, 1981.

[34] JIANG Ruo-chen, DAI Feng, LIU Yi, LI Ang. Fast marching method for microseismic source location in cavern-containing rockmass: Performance analysis and engineering application [J]. Engineering, 2021, 7: 1023−1034.

[35] GE Mao-chen. Optimization of transducer array geometry for acoustic emission/microseismic source location [D]. Pennsylvania, USA: The Pennsylvania State University, 1988.

[36] GE Mao-chen. Source location error analysis and optimization methods [J]. Journal of Rock Mechanics and Geotechnical Engineering, 2012, 4: 1−10.

[37] GE Mao-chen. Efficient mine microseismic monitoring [J]. International Journal of Coal Geology, 2005, 64: 44−56.

[38] LI Nan, GE Mao-chen, WANG En-yuan, ZHANG Shao-hua. The influence mechanism and optimization of the sensor network on the MS/AE source location [J]. Shock and Vibration, 2020, 2020: 2651214.

[39] LESNIAK A. Seismic network configuration by reduction of seismic source location errors [J]. International Journal of Rock Mechanics and Mining Sciences, 2015, 80: 118−128.

[40] LESNIAK A, PSZCZOLA G. Combined mine tremors source location and error evaluation in the Lubin Copper Mine (Poland) [J]. Tectonophysics, 2008, 456: 16−27.

[41] GE Mao-chen. Comparison of least squares and absolute value methods in Ae/MS source location: A case study [J]. International Journal of Rock Mechanics and Mining Sciences, 1997, 34: 93.e1−93.e7.

[42] KIJKO A. An algorithm for the optimum distribution of a regional seismic network — I [J]. Pure and Applied Geophysics, 1977, 115: 999−1009.

[43] KIJKO A. An algorithm for the optimum distribution of a regional seismic network—II. An analysis of the accuracy of location of local earthquakes depending on the number of seismic stations [J]. Pure and Applied Geophysics, 1977, 115: 1011−1021.

[44] GONG Si-yuan, DOU Lin-ming, MA Xiao-ping, MOU Zong-long, LU Cai-ping. Optimization algorithm of network configuration for improving location accuracy of microseism in coal mine [J]. Chinese Journal of Rock Mechanics and Engineering, 2012, 31: 8−17. (in Chinese)

[45] GONG Si-yuan, DOU Lin-ming, CAO An-ye, HE Hu, DU Tao-tao, JIANG Heng. Study on optimal configuration of seismological observation network for coal mine [J]. Chinese Journal of Geophysics, 2010, 53: 457−465. (in Chinese)

[46] MENDECKI A J. Seismic monitoring in Mines [M]. Dordrecht: Springer Science & Business Media, 1996.

[47] BONDAR I, MYERS S C, ENGDAHL E R, BERGMAN E A. Epicentre accuracy based on seismic network criteria [J]. Geophysical Journal International, 2004, 156: 483−496.

[48] EASA S M, HOSSAIN K M A. New mathematical optimization model for construction site layout [J]. Journal of Construction Engineering and Management, 2008, 134: 653−662.

[49] LIU Fei, MA Tian-hui, CHEN Feng. Prediction of rockburst in tunnels at the Jinping II hydropower station using microseismic monitoring technique [J]. Tunnelling and Underground Space Technology, 2018, 81: 480−493.

[50] LI Xi-bing, GONG Feng-qiang, TAO Ming, DONG Long-jun, DU Kun, MA Chun-de, ZHOU Zi-long, YIN Tu-bing. Failure mechanism and coupled static-dynamic loading theory in deep hard rock mining: A review [J]. Journal of Rock Mechanics and Geotechnical Engineering, 2017, 9: 767−782.

[51] LI L, TAN J Q, WOOD D A, ZHAO Z G, BECKER D, LYU Q, SHU B, CHEN H C. A review of the current status of induced seismicity monitoring for hydraulic fracturing in unconventional tight oil and gas reservoirs [J]. Fuel, 2019, 242: 195−210.

[52] ZHU Yi-qing, LIU Fang, ZHANG Guo-qing, XU Yun-ma. Development and prospect of mobile gravity monitoring and earthquake forecasting in recent ten years in China [J]. Geodesy and Geodynamics, 2019, 10: 485−491.

[53] WU Cheng-long, TIAN Xiao-bo, XU Tao, LIANG Xiao-feng, CHEN Yun, TAYLOR M, BADAL J, BAI Zhi-ming, DUAN Yao-hui, YU Gui-ping. Deformation of crust and upper mantle in central Tibet caused by the northward subduction and slab tearing of the Indian lithosphere: New evidence based on shear wave splitting measurements [J]. Earth and Planetary Science Letters, 2019, 514: 75−83.

[54] LU Zhen-hua, ZHANG Lian-cheng. Evaluation of near-field monitoring efficiency of tremsers in mentougou mine [J]. Earthquake, 1989, 5: 32−39. (in Chinese)

[55] LI Shu-lin, YIN Xian-gang, ZHENG Wen-da, CEZAR T. Research of multi-channel microseismic monitoring system and its application to fankou lead-zinc mine [J]. Chinese Journal of Rock Mechanics and Engineering, 2005, 24: 2048−2053. (in Chinese)

[56] TANG Li-zhong, PAN Chang-liang, YANG Cheng-xiang, GUO Ran. Establishment and application of microseismicity monitoring system in dongguashan copper mine [J]. Metal Mine, 2006, 10: 41−44. (in Chinese)

[57] LI Pan-yu, MEI Fu-ding, HE Zou-jun, ZHOU Ke-li, LUO Wei-bing. Study on establishment and application of microseismic monitoring system in Tonglushan mine [J]. China Ming Magazine, 2020, 29: 82−87. (in Chinese)

[58] REN Chao-fa, ZHAO Hai-bo, CHEN Bai-jun, FENG Cheng-bin, ZHANG Sheng-rui. Analysis of location precision factors in surface microseismic monitoring acquisition geometry: A case study of an SZ exploration area in Daqing, China [J]. Geophysical Prospecting for Petroleum, 2018, 57: 668−677. (in Chinese)

[59] MENG Zhao-ping, WANG Yu-heng, ZHANG Kun, LU Yi-xin, CHEN Jun, YAO Meng. Analysis of hydraulic fracturing cracks for coal reservoirs and in-situ stressdirection in Southern Qinshui Basin [J]. Coal Science & Technology, 2019, 47: 216−222. (in Chinese)

[60] ZHAO Yan-hong, ZHANG Fan, SU Ya-mei. Influence of station layout on earthquake location of inner Mongolia seismic network [J]. Seismological and Geomagnetic Observation and Research, 2018, 39: 88−95. (in Chinese)

[61] WEI Yong-gang. The function and layout of the Norwegian seismic array (NORSAR) [J]. Seismological and Geomagnetic Observation and Research, 2020, 41: 137−143. (in Chinese)

[62] CHEN Hai-long, LI Hai-feng, LI Zhao-min, LI Song-yan, WANG Yu-jun, WANG Jian, LI Bin-fei. Effects of matrix permeability and fracture on production characteristics and residual oil distribution during flue gas flooding in low permeability/tight reservoirs [J]. Journal of Petroleum Science and Engineering, 2020, 195: 107813.

[63] BARTHWAL H, VAN DER BAAN M. Role of fracture opening in triggering microseismicity observed during hydraulic fracturing [J]. Geophysics, 2019, 84: KS105−KS118.

[64] YU Hai-yang, YANG Zhong-lin, LUO Le, LIU Jun-hui, CHENG Shi-qing, QU Xue-feng, LEI Qi-hong, LU Jun. Application of cumulative-in-situ-injection-production technology to supplement hydrocarbon recovery among fractured tight oil reservoirs: A case study in Changqing Oilfield, China [J]. Fuel, 2019, 242: 804−818.

[65] ZHANG Liang, REN Bo, HUANG Hai-dong, LI Yong-zhao, REN Shao-ran, CHEN Guo-li, ZHANG Hua. CO_2 EOR and storage in Jilin oilfield China: Monitoring program and preliminary results [J]. Journal of Petroleum Science and Engineering, 2015, 125: 1−12.

[66] REN Bo, REN Shao-ran, ZHANG Liang, CHEN Guo-li, ZHANG Hua. Monitoring on CO_2 migration in a tight oil reservoir during CCS-EOR in Jilin Oilfield China [J]. Energy, 2016, 98: 108−121.

[67] ZHANG Yong-hua, CHEN Xiang, YANG Dao-qing, ZHAO Yu-qing, GUO Jin-rong. The application of micro-seismic monitoring technology to the study of horizontal well fracturing [J]. Geophysical & Geochemical Exploration, 2013, 37: 1080−1084. (in Chinese)

[68] LIU Ying, ZHANG Hai-jiang, FANG Hong-jian, YAO Hua-jian, GAO Ji. Ambient noise tomography of three-dimensional near-surface shear-wave velocity structure around the hydraulic fracturing site using surface microseismic monitoring array [J]. Journal of Applied Geophysics, 2018, 159: 209−217.

[69] KRAFT T, MIGNAN A, GIARDINI D. Optimization of a large-scale microseismic monitoring network in northern Switzerland [J]. Geophysical Journal International, 2013, 195: 474−490.

[70] ZHAO Pei. Research on local scale region microseism location based on high density stations [D]. Fuxin: Liaoning Technical University, 2016. (in Chinese)

[71] LIU Ya-lei, GU Xiao-hui, LIAN Yun-meng, LIU Heng. Optimal arrangement of four-sensor dynamic acoustic array [J]. Sensor Review, 2012, 32: 288−295.

[72] BAXTER M G, PULLIN R, HOLFORD K M, EVANS S L. Delta T source location for acoustic emission [J]. Mechanical Systems and Signal Processing, 2007, 21: 1512−1520.

[73] DOWNS A, ROBERTS R, SONG Ji-ming. Array based guided wave source location using dispersion compensation [J]. Journal of Nondestructive Evaluation, Diagnostics and Prognostics of Engineering Systems, 2021, 4: 041002.

[74] MO Bi-ming, LI Jian, KONG Hui-hua, XIN Wei-yao, HE Ming. Optimization method of shock sensor array layouts based on FK beam forming [J]. Computer Measurement & Control, 2019, 27: 285−288, 293. (in Chinese)

[75] ROSACINTAS S, GALIANAMERINO JJ, ALFARO P, ROSAHERRANZ J. Optimizing the number of stations in arrays measurements: Experimental outcomes for different array geometries and the f–k method [J]. Journal of Applied

Geophysics, 2014, 102: 96−133.
[76] OKADA H. Theory of efficient array observations of microtremors with special reference to the SPAC method [J]. Exploration Geophysics, 2006, 37: 73−85.
[77] ASTEN M W. Array estimators and the use of microseisms for reconnaissance of sedimentary basins [J]. Geophysics, 1984, 15: 1828−1837.
[78] ASTEN M W. On bias and noise in passive seismic data from finite circular array data processed using SPAC methods [J]. Geophysics, 2006, 71: V153−V162.
[79] ARORA S K, VARGHESE T G, BASU T K. Relative performance of different triangular networks in locating regional seismic sources [J]. Proceedings of the Indian Academy of Sciences — Section A, Earth and Planetary Sciences, 1978, 87: 271−281.
[80] DENG Min-de. Study on optimal layout of regional seismograph network [J]. Seismic and Geomagnetic Observation and Research, 1988, 2: 35−39. (in Chinese)
[81] ALJETS D, CHONG A, WILCOX S, HOLFORD K. Acoustic emission source location on large plate-like structures using a local triangular sensor array [J]. Mechanical Systems & Signal Processing, 2012, 30: 91−102.
[82] KIJKO A, SCIOCATTI M. Optimal spatial distribution of seismic stations in mines [J]. International Journal of Rock Mechanics and Mining Sciences & Geomechanics Abstracts, 1995, 32: 607−615.
[83] CHEN Ting, HUANG Lian-jie. Optimal design of microseismic monitoring network: Synthetic study for the Kimberlina CO_2 storage demonstration site [J]. International Journal of Greenhouse Gas Control, 2020, 95: 102981.
[84] DONG Long-jun, LI Xi-bing, TANG Li-zhong, GONG Feng-qiang. Mathematical functions and parameters for Microseismic source location without pre-measuring speed [J]. Chinese Journal of Rock Mechanics and Engineering 2011, 30: 2057−2067. (in Chinese)
[85] DONG Long-jun, LI Xi-bing. Three-dimensional analytical solution of acoustic emission or microseismic source location under cube monitoring network [J]. Transactions of Nonferrous Metals Society of China, 2012, 22: 3087−3094.
[86] DONG Long-jun, LI Xi-bing, ZHOU Zi-long, CHEN Guang-hui, MA Ju. Three-dimensional analytical solution of acoustic emission source location for cuboid monitoring network without pre-measured wave velocity [J]. Transactions of Nonferrous Metals Society of China, 2015, 25: 293−302.
[87] PADOIS T, DOUTRES O, SGARD F, BERRY A. Optimization of a spherical microphone array geometry for localizing acoustic sources using the generalized cross-correlation technique [J]. Mechanical Systems and Signal Processing, 2019, 132: 546−559.
[88] STEINBERG D M, RABINOWITZ N, SHIMSHONI Y, MIZRACHI D. Configuring a seismographic network for optimal monitoring of fault lines and multiple sources [J]. Bulletin of the Seismological Society of America, 1995, 85: 1847−1857.
[89] ARTEMIEVA I M, BILLIEN M, LEVEQUE J J, MOONEY W D. Shear wave velocity, seismic attenuation, and thermal structure of the continental upper mantle [J]. Geophysical Journal International, 2004, 157: 607−628.
[90] COOPER R F. Seismic wave attenuation: Energy dissipation in viscoelastic crystalline solids [J]. Reviews in Mineralogy and Geochemistry, 2002, 51: 253−290.

传感器阵列对岩体微震/声发射源定位精度的影响

黄麟淇，吴 欣，李夕兵，王少锋

中南大学 资源与安全工程学院，长沙 410083

摘 要：随着开采深度增加，岩体动力灾害日益突出。微震监测已成为岩爆、顶板坍塌等岩体动力灾害监测的重要技术手段。传感器阵列布设作为信号采集的第一步，严重影响信号源的定位精度。讨论和总结有关由传感器阵列布设引起的微震(MS)和声发射(AE)震源定位误差的重要研究，并分析传感器数量、传感器布设形态以及传感器与震源距离对 MS/AE 源定位精度的影响机制。随后，结合工程实践和实验室测试，给出传感器阵列的一些布设原则，并通过现场应用进行验证。另外，综合考虑影响传感器阵列布设数量、形状和距离的因素，找到最优布置方案，可大幅度改善信号采集效果，提高信号源定位精度。最后，对提高 MS/AE 源定位精度所面临的挑战和传感器阵列方面相应的应对策略进行展望。

关键词：微震监测；声发射；传感器阵列；源定位精度

(Edited by Sai-qian YUAN)